9-2011

Hydrogen Donors and Ti^{3+} ions in reduced TiO_2 crystals

A. T. Brant
West Virginia University

Shan Yang (杨山)
West Virginia University

Nancy C. Giles
Air Force Institute of Technology

Larry E. Halliburton
West Virginia University

Recommended Citation

Brant, A. T., Giles, N. C., & Halliburton, L. E. (2011). Hydrogen donors and Ti 3+ ions in reduced TiO 2 crystals. Journal of Applied Physics, 110(5), 053714. https://doi.org/10.1063/1.3630964

Journal of Applied Physics

AIP Publishing

RESEARCH ARTICLE | SEPTEMBER 14 2011

Hydrogen donors and Ti^{3+} ions in reduced TiO_2 crystals

A. T. Brant; Shan Yang (杨山); N. C. Giles; L. E. Halliburton

Journal of Applied Physics 110, 053714 (2011)

https://doi.org/10.1063/1.3630964

JOURNAL OF APPLIED PHYSICS **110**, 053714 (2011)

Hydrogen donors and Ti^{3+} ions in reduced TiO_2 crystals

A. T. Brant,[1] Shan Yang(杨山),[1] N. C. Giles,[2] and L. E. Halliburton[1,a)]
[1]*Department of Physics, West Virginia University, Morgantown, West Virginia 26506, USA*
[2]*Department of Engineering Physics, Air Force Institute of Technology, Wright-Patterson Air Force Base, Ohio 45433, USA*

(Received 16 June 2011; accepted 19 July 2011; published online 14 September 2011)

Electron paramagnetic resonance (EPR) and electron-nuclear double resonance (ENDOR) are used to identify and characterize the neutral hydrogen donor in TiO_2 crystals having the rutile structure. These spectra are best observed near 5 K. The neutral donors are present without photoexcitation in crystals that have been slightly reduced at high temperature in a nitrogen atmosphere. The same defects can be photoinduced at low temperature in oxidized crystals. The neutral hydrogen donor in this lattice consists of a substitutional Ti^{3+} ion adjacent to a substitutional OH^- molecular ion. The axis of the OH^- molecule lies in the basal plane with the hydrogen ion extending out from the oxygen in a direction perpendicular to the Ti-O bonds. Spin-Hamiltonian parameters are obtained from the angular dependence of the EPR and ENDOR spectra (principal values are 1.9732, 1.9765, and 1.9405 for the g matrix and –0.401, +0.616, and –0.338 MHz for the ^1H hyperfine matrix). The principal axis associated with the +0.616 MHz principal value is in the basal plane 22.9° from a [110] direction and the principal axis associated with the –0.338 MHz principal value is along the [001] direction. Our results show that interstitial Ti^{3+} ions are not the dominant shallow donors in slightly reduced TiO_2 (rutile) crystals. © *2011 American Institute of Physics.*
[doi:10.1063/1.3630964]

I. INTRODUCTION

The Ti^{3+} ($3d^1$) ion is the most often cited defect in titanium dioxide (TiO_2) crystals. These electron traps are important shallow donors and their properties and location in the lattice have been widely discussed.[1–5] A continuing basic question is whether they occupy substitutional or interstitial sites. Although some investigators refer to a generic Ti^{3+} defect, a large number of different Ti^{3+} centers have been observed in TiO_2 (rutile) crystals. Despite having been studied since the early 1960s,[6–10] only recently have detailed models been firmly established for the most prominent of these Ti^{3+} centers.[11–14] Electron paramagnetic resonance (EPR) and electron-nuclear double resonance (ENDOR) techniques are well suited to study these paramagnetic point defects in bulk TiO_2 crystals.[15] The Ti^{3+}-related defects normally have $S = 1/2$ and their EPR spectra do not exhibit complex crystal field effects. Also, the widths of the EPR lines are usually small because of the lack of broadening due to hyperfine interactions. This results in well-resolved Ti^{3+} spectra in strain-free TiO_2 crystals. Magnetic isotopes of the host elements have low abundances (^{47}Ti has $I = 5/2$ and is 7.4% abundant, ^{49}Ti has $I = 7/2$ and is 5.4% abundant, and ^{17}O has $I = 5/2$ and is 0.038% abundant). Many of the Ti^{3+} centers have long spin-lattice relaxation times at low temperature and thus are good candidates for ENDOR experiments where saturation of the EPR signal is an important requirement.

In the present paper, results obtained from EPR and ENDOR experiments show that the "neutral hydrogen donor" in TiO_2 (rutile) crystals consists of a substitutional Ti^{3+} ion next to a substitutional OH^- molecular ion. Our shallow donor model in this partially ionic material differs significantly from the classic shallow donor in tetrahedrally bonded covalent semiconductors where the electron is centered at an impurity and occupies a delocalized hydrogenic state. Instead, our model for the neutral hydrogen donor is similar to that previously developed for the neutral fluorine donor in TiO_2 crystals.[13] Infrared absorption shows that significant amounts of hydrogen, in the form of isolated OH^- ions, are present in as-grown fully oxidized TiO_2 (rutile) bulk crystals. An isolated OH^- defect, representing a singly ionized hydrogen donor, is converted to a neutral hydrogen donor in these crystals when an electron is localized on a neighboring titanium ion. Neutral hydrogen donors can be temporarily produced in oxidized crystals (having midgap Fermi levels) by photoexcitation at low temperature. Conversely, neutral hydrogen donors are present without photoexcitation in crystals reduced in nitrogen atmospheres at high temperature (and thus having higher Fermi levels). The principal values and directions of the principal axes for the g matrix and the ^1H hyperfine matrix are obtained from the EPR and ENDOR spectra. These spin-Hamiltonian parameters establish the ground-state model of the neutral hydrogen donor in TiO_2 (rutile).

Our results provide resolution to a lengthy debate in the literature about the identity of the primary donor produced during a slight reduction of bulk TiO_2 crystals. They also complement the recent detailed study of the infrared absorption properties of hydrogen in TiO_2 by Herklotz *et al.*[16] The EPR spectrum described in the present study corresponds to the A center reported in 1961 by Chester.[6] We demonstrate

---

[a)] Author to whom correspondence should be addressed: Larry.Halliburton@mail.wvu.edu.

that hydrogen is an integral part of the A center and thus provide a strong argument against the assignment of Chester's A center to an interstitial Ti^{3+} ion. Based on our EPR and ENDOR data, we conclude that the A center in TiO_2 (rutile) is the neutral hydrogen donor where the unpaired spin is localized primarily on a neighboring titanium ion instead of being centered on the hydrogen in a diffuse wave function.

II. EXPERIMENTAL DETAILS

The TiO_2 crystals used in this investigation have the rutile structure and were obtained from CrysTec (Berlin, Germany) and MTI Corporation (Richmond, CA). EPR-sized samples with dimensions of $1.5 \times 4 \times 2$ mm^3 and $2 \times 3.5 \times 1$ mm^3 were cut from the larger [001] plates provided by CrysTec and MTI, respectively. The optical and magnetic resonance results were similar from the two TiO_2 samples. Hydrogen was found to be an unintentional impurity in both crystals. The as-received crystals were colorless at room temperature and did not exhibit EPR signals from Ti^{3+} ions,[11] thus indicating that they were fully oxidized. The only EPR signals observed in the as-received crystals were from substitutional singly ionized Fe^{3+} and Cr^{3+} acceptors. During the reducing treatments, a quartz tube containing flowing nitrogen gas extended through a horizontal furnace. A sample was inserted into the flowing nitrogen gas after the set temperature was reached, and was quickly removed (returning to room temperature within seconds) at the end of the heating period. Data are reported from two reduced samples: one was held at 600 °C for 10 min and the other was held at 650 °C for 50 min. The same hydrogen-related EPR and ENDOR signals were observed in the two reduced samples.

Infrared absorption data were taken with a Nicolet 8700 FT-IR spectrometer, EPR data were taken with a Bruker EMX spectrometer, and ENDOR data were taken with a Bruker Elexsys E-500 spectrometer. Oxford helium-gas-flow systems provided temperature control for all three spectrometers. The magnetic resonance spectrometers operated near 9.4 GHz. Proton NMR gaussmeters were used to measure the static magnetic fields and a Cr-doped MgO crystal was used to correct for the small difference in magnetic field between the sample and the probe tip of the gaussmeter (the isotropic g value for $MgO:Cr^{3+}$ is 1.9800). A He-Cd laser providing 15 mW of 442 nm light was used to illuminate samples at low temperature in the EPR microwave cavity.

III. RESULTS

A. Infrared absorption

Figure 1 shows the infrared absorption spectra obtained from the TiO_2 crystal that had been reduced for 10 min at 600 °C in a nitrogen atmosphere. These data were taken at room temperature (trace a) and 10 K (trace b) with unpolarized light propagating along the [001] direction in the crystal. At room temperature, the peak occurs at 3277.6 cm^{-1} and its full width at half-maximum is 14.7 cm^{-1}. At 10 K, the peak shifts to 3287.5 cm^{-1} and the width reduces to 2.9 cm^{-1}. The same OH^- band, smaller by about a factor of two, was observed in this crystal before the reduction, thus demonstrating that a substantial portion of the hydrogen was present in the crystal before the reducing treatment. This result suggests that hydrogen is easily incorporated in TiO_2 crystals during growth and implies that many as-grown crystals will contain significant concentrations of hydrogen. The absorption band in Fig. 1 is assigned to isolated OH^- molecular ions (i.e., the OH^- ions are not adjacent to other point defects in the TiO_2 lattice).[16–22] These earlier studies showed that the OH^- band is highly polarized with the electric dipole axis (i.e., the bond direction) oriented in the basal plane of the crystal. We estimate the approximate concentration of OH^- ions in our slightly reduced crystal to be 8×10^{17} cm^{-3}. This value was obtained by combining the room-temperature data in Fig. 1 with the absorption strength per ion determined earlier by Johnson *et al.*[23]

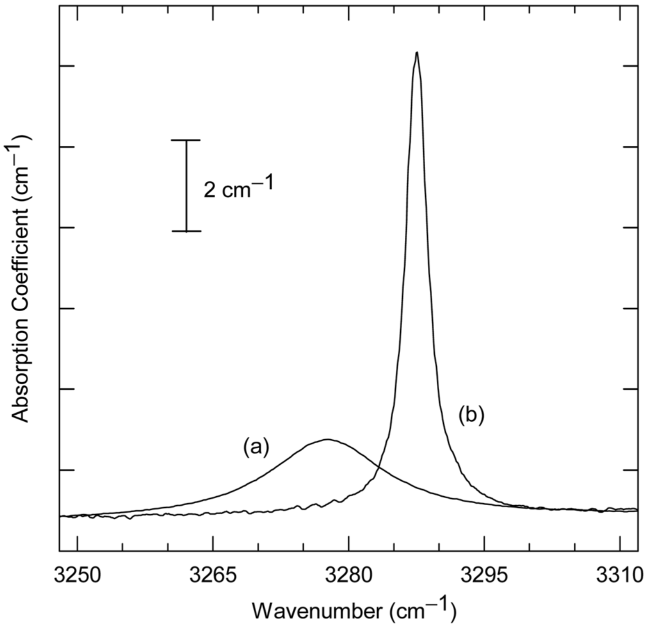

FIG. 1. Infrared absorption of OH^- molecular ions in a slightly reduced TiO_2 (rutile) crystal. Trace (a) was obtained at room temperature and trace (b) was obtained at 10 K. Data were taken with unpolarized light propagating along the [001] direction in a 2 mm thick crystal.

B. Electron paramagnetic resonance

Reducing a TiO_2 crystal at 600 °C for 10 min in a nitrogen atmosphere produced the EPR signals shown in Fig. 2. The signals were not present before the reduction. These data were taken at 5 K with the magnetic field along the [001] direction in the crystal. Above 10 K, the primary EPR signal in Fig. 2 broadens and becomes difficult to detect as the increasing conductivity of the reduced sample causes the sensitivity of the spectrometer to deteriorate (i.e., the Q of the microwave cavity decreases significantly at higher temperature). Small lines on the low-field side of the primary line in Fig. 2 are due to Nb^{4+} centers.[24,25] The weak lines on the high-field side are caused by unidentified defects in the TiO_2 crystal. Figure 3 shows EPR spectra from the primary defect when the magnetic field is in the basal plane. The magnetic field is along the [100] direction in Fig. 3(a), the

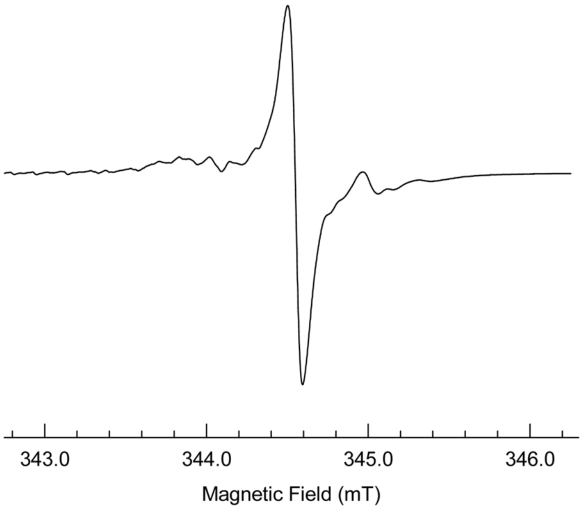

FIG. 2. EPR spectrum of the neutral hydrogen donor in a slightly reduced TiO_2 (rutile) crystal. These data were taken at 5 K with the magnetic field along the [001] direction. The microwave frequency was 9.3719 GHz.

field is 30° from the [100] direction in Fig. 3(b), and the field is along the [110] direction in Fig. 3(c). The major EPR lines in Figs. 2 and 3 have widths between 0.06 and 0.10 mT and show no resolved hyperfine splittings for these or any other orientations of the magnetic field. A series of ENDOR experiments described in Sec. III C, however, show that a small unresolved hyperfine interaction with hydrogen is present in these EPR lines (^1H has $I = 1/2$ and is 99.985% abundant). Thus, we assign these EPR lines to the neutral hydrogen donor in TiO_2 (rutile).

We also found that the neutral hydrogen donor EPR signals in Figs. 2 and 3 can be produced in a fully oxidized as-received TiO_2 crystal during an exposure to 442 nm laser light at 5 K. In this alternative mode of production, self-trapped hole centers[14] are the source of photoexcited electrons that temporarily convert the singly ionized hydrogen donors to their neutral paramagnetic charge state at very low temperatures. A similar behavior was observed for neutral fluorine donors in TiO_2 crystals.[13]

The model of the ground state of the neutral hydrogen donor is illustrated in Fig. 4. There are two equivalent distorted TiO_6 octahedra in the TiO_2 rutile lattice (the basal plane of one of these TiO_6 units is shown in Fig. 4). The two TiO_6 units are elongated in directions perpendicular to the [001] direction with the six oxygen ions within a unit separating into a set of two along the elongation direction and a set of four in the plane perpendicular to the elongation direction. The two octahedra are related by a 90° rotation about the [001] direction. In the model in Fig. 4, an OH^- ion with its unique axis along the $[\bar{1}10]$ direction in the basal plane is located at one of the two oxygen positions along the elongation direction and is adjacent to a substitutional Ti^{3+} ion. The unpaired spin is primarily localized on the titanium, thus forming the Ti^{3+} ($3d^1$) ion and explaining the small hyperfine interaction with the hydrogen nucleus. There are four possible crystallographically equivalent locations of the H^+ ion around the Ti^{3+} ion in Fig. 4 (in EPR studies, different

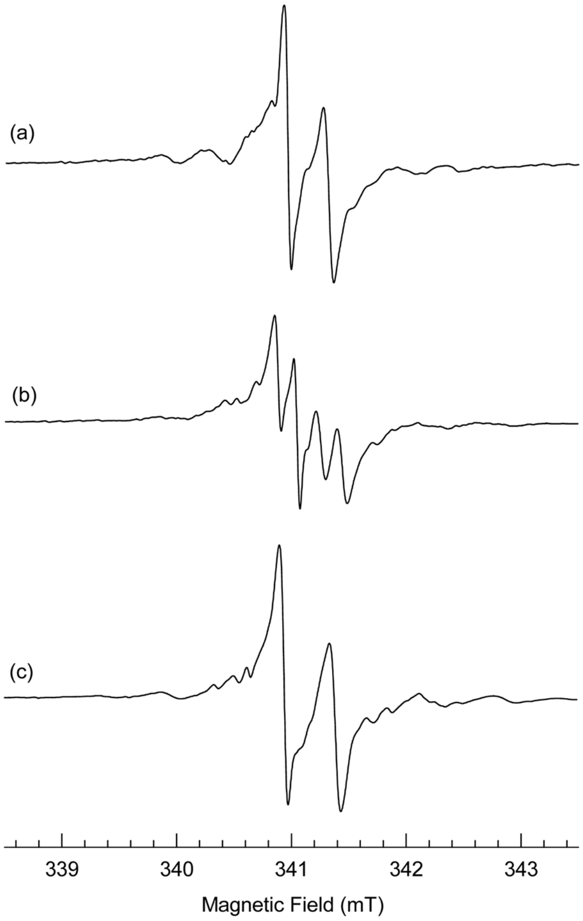

FIG. 3. EPR spectra of the neutral hydrogen donor in the reduced TiO_2 crystal. These data were taken at 5 K with the magnetic field in the basal plane. The microwave frequency was 9.4443 GHz. (a) Magnetic field along the [100] direction. (b) Magnetic field 30° from the [100] direction. (c) Magnetic field along the [110] direction.

orientations of a defect are usually referred to as different sites of the defect). These four sites correspond to the proton (H^+) extending out from the oxygen in either the $[\bar{1}10]$ or $[1\bar{1}0]$ directions for each of the two oxygen locations along the [110] elongation direction. The other TiO_6 unit in the lattice, rotated by 90°, gives a second set of four crystallographically equivalent sites for this defect. Thus, there are a total of eight crystallographically equivalent sites (i.e., orientations) of the neutral hydrogen donor in the TiO_2 (rutile) lattice. Because of their pairwise nature, only four of these crystallographically equivalent sites will be separately observed in an EPR spectrum taken with the magnetic field along an arbitrary direction in the crystal.

The eight crystallographically equivalent sites of the neutral hydrogen donor are all magnetically equivalent when the magnetic field is along the [001] direction, thus giving the one EPR line shown in Fig. 2. When the magnetic field is along the [100] or [110] direction, the eight crystallographically equivalent sites separate into two sets of four. The two sets are magnetically inequivalent, thus giving two EPR lines for each of these directions of magnetic field, as shown in

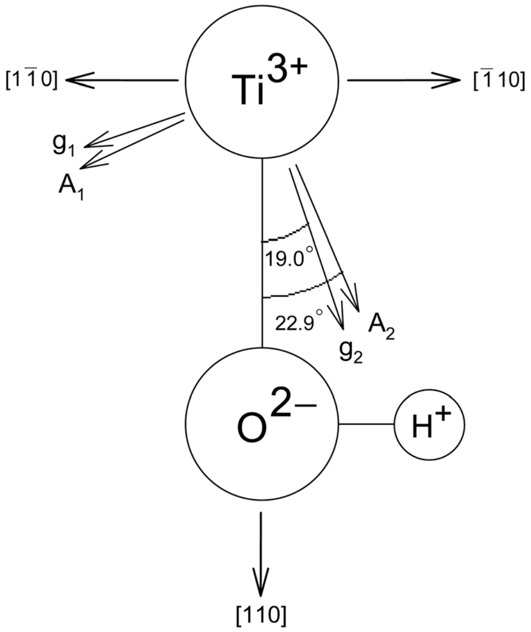

FIG. 4. Model of the neutral hydrogen donor in TiO_2 illustrating the localization of the unpaired electron on a neighboring titanium ion. This is a projection on the (001) plane. The g_3 and A_3 principal axes are along the [001] direction.

Figs. 3(a) and 3(c). There are two magnetically inequivalent sets of sites (and thus two EPR lines) when the magnetic field is rotated in the (010) plane from the [001] to [100] direction. Rotation in the ($\bar{1}$10) plane from [001] to [110] also gives two EPR lines. In contrast, rotation of the field in the (001) plane between [100] and [110] gives four magnetically inequivalent sets of sites (with two sites in each set) and thus four EPR lines, as illustrated in Fig. 3(b).

The following spin Hamiltonian was used to determine the g matrix of the neutral hydrogen donor.

$$\mathbf{H} = \beta \mathbf{S} \cdot \mathbf{g} \cdot \mathbf{B}. \tag{1}$$

The direction of one principal axis of the g matrix must be along the [001] direction, as this is a turning point in the EPR angular dependence. The directions of the two remaining principal axes must be in the basal plane, but neither is along a high-symmetry [100] or [110] direction. Thus, four parameters are required to describe the g matrix (three principal values and one angle to specify the directions of the two principal axes in the basal plane). EPR spectra taken along the [100], [110], and [001] directions were used to obtain the "best-fit" values for these four parameters. Our least-squares fitting procedure involved a series of diagonalizations of the 2×2 Hamiltonian matrix ($S = 1/2$). Input data consisted of 5 magnetic field values and their associated microwave frequencies. These included one line from the [001] spectrum in Fig. 2, two lines from the [100] spectrum in Fig. 3(a), and two lines from the [110] spectrum in Fig. 3(b). Final "best-fit" values of the four parameters describing the g matrix are listed in Table I. EPR data were also taken at other orientations of magnetic field and used to verify the correctness of the g matrix parameters in Table I. For comparison, the values obtained by Chester[6] for the A center g matrix were 1.974, 1.977, 1.941, and 19° from the [110] direction. The angular dependence of the EPR spectrum in the (1$\bar{1}$0) and (001) planes is shown in Fig. 5.

TABLE I. Spin-Hamiltonian parameters for one orientation (i.e., site) of the neutral hydrogen donor in a TiO_2 (rutile) crystal. For the defect described below, the distorted TiO_6 octahedron is elongated along the [110] direction and the hydrogen bond extends in the [$\bar{1}$10] direction. The model of this defect is shown in Fig. 4. Directions of the principal axes for g_1, g_2, A_1, and A_2 are in the (001) plane. The uncertainty in the angles specifying these directions in the basal plane is estimated to be ±2°.

Matrix type	Principal value	Principal-axis direction
g matrix		
g_1	1.9732 ± 0.0002	19.0° from [1$\bar{1}$0]
g_2	1.9765 ± 0.0002	19.0° from [110]
g_3	1.9405 ± 0.0002	[001]
hydrogen hyperfine matrix		
A_1	–0.401 MHz ± 0.01 MHz	22.9° from [1$\bar{1}$0]
A_2	+0.616 MHz ± 0.01 MHz	22.9° from [110]
A_3	–0.338 MHz ± 0.01 MHz	[001]

A previous analysis[13] of the g matrix for the neutral fluorine donor in TiO_2 (rutile) suggested that the unpaired d electron on the primary Ti^{3+} ion occupies a $|x^2 - y^2\rangle$ orbital. The principal values of the g matrices for the hydrogen and fluorine neutral donors are similar. Thus, we suggest that the unpaired d electron on the primary Ti^{3+} ion also occupies a $|x^2 - y^2\rangle$ orbital in the neutral hydrogen donor in TiO_2. Referring to Fig. 4, the x, y, z coordinate system used to describe this occupied orbital has x along the [$\bar{1}$10] direction, y along the [001] direction, and z along the [110] direction.

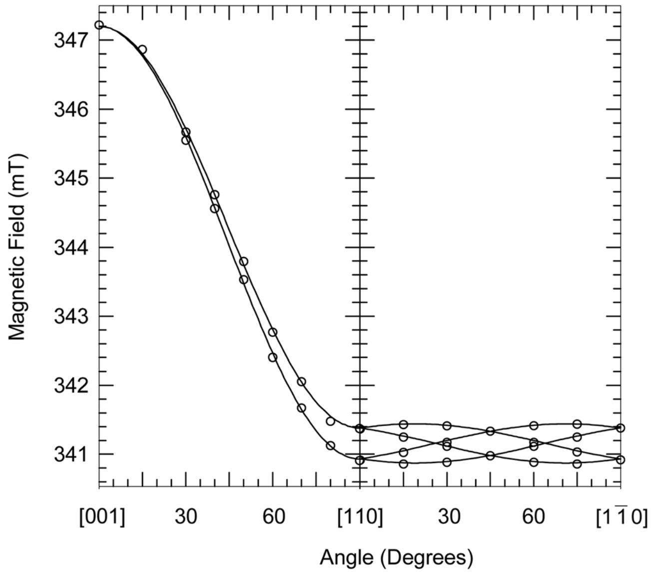

FIG. 5. EPR angular dependence of the neutral hydrogen donor in the (1$\bar{1}$0) and (001) planes. The solid lines were generated using the g-matrix parameters in Table I and a microwave frequency of 9.430 GHz. The discrete points are experimental results.

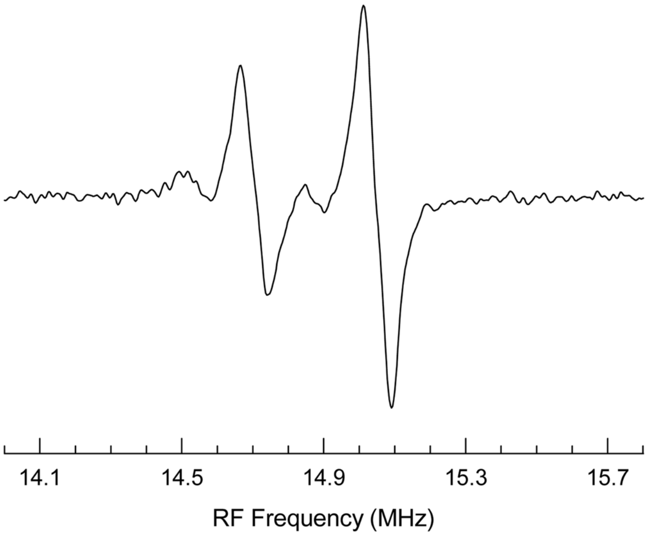

FIG. 6. ENDOR spectrum from the neutral hydrogen donor in a slightly reduced TiO_2 crystal. Data were taken at 5 K with the magnetic field parallel to the [001] direction.

C. Electron-nuclear double resonance

Figure 6 shows the ENDOR spectrum from the neutral hydrogen donor in TiO_2 (rutile) when the magnetic field is along the [001] direction. These data were taken at 5 K from the sample that had been reduced at 650 °C for 50 min. The two large lines in Fig. 6 are separated by 0.338 MHz and are centered on 14.877 MHz. Their linewidths are approximately 80 kHz. For a weak hyperfine interaction, the first-order ENDOR spectrum from an $I = 1/2$ nucleus contains two lines that are separated by the hyperfine parameter A and centered on the Larmor frequency ν_N (where $\nu_N = g_N\beta_N B/h$). The ENDOR spectrum in Fig. 6 was taken at a magnetic field of 349.088 mT, where the known value[26] of ν_N for a ^1H nucleus is 14.863 MHz. This known value of ν_N for ^1H falls very near the center of the two lines in Fig. 6, thus proving that a ^1H nucleus (i.e., a proton) is responsible for the hyperfine splitting observed in the [001] ENDOR spectrum. The smaller ENDOR line (at 14.868 MHz) between the two large lines in Fig. 6 is due to "distant" hydrogen nuclei in the lattice. The ENDOR line at 14.548 MHz on the low-frequency side of the spectrum in Fig. 6 is part of a pair of lines representing a weak hydrogen hyperfine interaction associated with a different and less intense EPR signal that underlies our primary EPR signal in Fig. 2. The high-frequency component of this pair is near 15.19 MHz and is barely observed. The identity of the secondary, underlying hydrogen-related defect is not known.

The ENDOR spectra in Figs. 7(a) and 7(b) were taken with the magnetic field along the [100] direction. These data were taken at 5 K from the sample that had been reduced at 600 °C for 10 min. In Fig. 7(a), the magnetic field is set at 339.997 mT, corresponding to the low-field EPR line in Fig. 3(a). The ENDOR lines are separated by 0.257 MHz and are centered on 14.475 MHz. In Fig. 7(b), the magnetic field is set at 340.274 mT, corresponding to the high-field line in Fig. 3(a). The ENDOR lines are separated by 0.473 MHz and are centered on 14.489 MHz. Both pairs of ENDOR lines in Fig. 7 are centered on the Larmor frequency ν_N for the ^1H nucleus, thus providing additional direct evidence that hydrogen is a primary component of this paramagnetic defect.

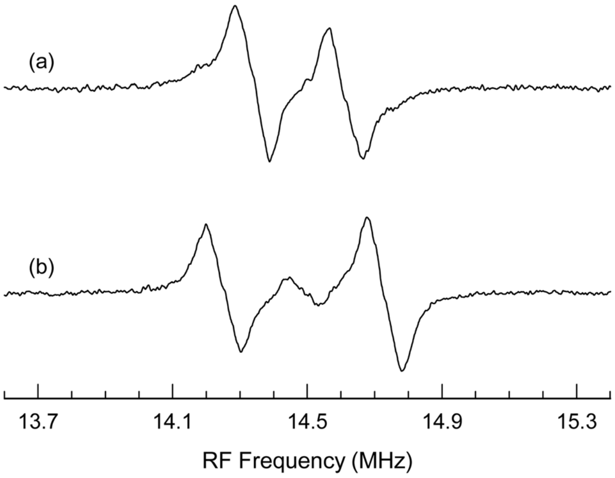

FIG. 7. ENDOR spectra from the neutral hydrogen donor taken at 5 K with the magnetic field parallel to the [100] direction. (a) ENDOR spectrum taken from the low-field EPR line. (b) ENDOR spectrum taken from the high-field EPR line.

The following spin Hamiltonian with electron Zeeman, hyperfine, and nuclear Zeeman terms was used to analyze the ENDOR data.

$$\mathbf{H} = \beta \mathbf{S}\cdot\mathbf{g}\cdot\mathbf{B} + \mathbf{I}\cdot\mathbf{S}\cdot\mathbf{A} - g_N\beta_N \mathbf{I}\cdot\mathbf{B}. \qquad (2)$$

Final values for the hyperfine parameters were obtained from a least-squares fitting procedure that involved exact diagonalizations of the 4×4 Hamiltonian matrix ($S = 1/2$, $I = 1/2$). Input data consisted of 10 ENDOR frequencies and their associated magnetic field values. These included two lines from the [001] spectrum in Fig. 6, four lines from the [100] spectra in Fig. 7, and four lines from the [110] spectra (not shown). Only four parameters were varied (three principal values and one angle). The direction of one principal axis of the *A* matrix must be along the [001] direction, as this is a turning point in the ENDOR angular dependence. The directions of the two remaining principal axes of the *A* matrix must be in the basal plane, but not along high-symmetry directions. During the ENDOR fitting, the *g* matrix parameters were not varied. The "best fit" values of the four parameters describing the *A* matrix are listed in Table I. The correctness of this final set of hyperfine parameters was verified by taking ENDOR data at additional orientations of the magnetic field in the basal plane. Only the relative signs of the hyperfine principal values were obtained from the experimental data. In Table I, we have chosen the set of signs that give a positive value for the dipole-dipole contribution to the *A* matrix. Figure 8 illustrates the angular dependence of the ^1H ENDOR spectra for rotations of the magnetic field from [001] to [100] and from [100] to [110]. As can be seen in Table I and Fig. 4, the directions of the principal axes for the *g* and *A* matrices are similar. The principal hyperfine axis pointing toward the hydrogen nucleus in Fig. 4 is assigned to the + 0.616 MHz principal value (i.e., the largest parameter).

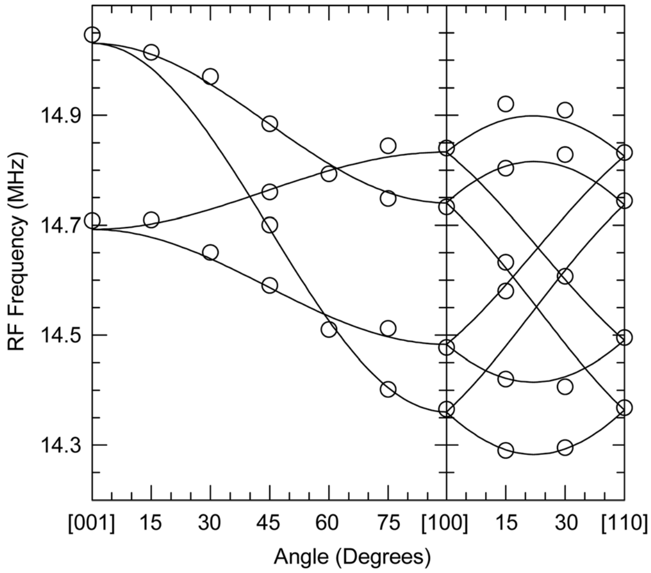

FIG. 8. ENDOR angular dependence of the neutral hydrogen donor in the (010) and (001) planes. The solid lines were generated using the hyperfine parameters in Table I and a microwave frequency of 9.480 GHz. The discrete points are experimental results.

Our results in Table I give a value of –0.041 MHz for the isotropic portion (i.e., Fermi contact term) of the hydrogen hyperfine matrix. We expect that the anisotropic portion of the hyperfine matrix sensitively reflects the distribution of the unpaired electron spin on the primary titanium ion, the six nearest-neighbor oxygen ions, and perhaps the second shell of titanium ions.

IV. DISCUSSION

The EPR signals that we investigate in the present paper were initially reported by Chester.[6] Our *g* matrix parameters (see Table I) are consistent with his A center values. In that early work, EPR data showed that the responsible defect was a Ti^{3+} ion with four distinguishable orientations within the TiO_2 (rutile) lattice. Although Chester proposed four possible models for his A center, several investigators[27–29] immediately embraced the Ti^{3+} interstitial model and this has become, for many, the *de facto* model of the dominant shallow donor in slightly reduced TiO_2 crystals. To quote from Shen et al.,[8] "*The alternative models of Chester, including that of an unknown center involving hydrogen, were not so much eliminated as ignored.*" The Ti^{3+} interstitial model found favor because it could provide a simple, plausible explanation of why the directions of the *g*-matrix principal axes in the basal plane were not along high symmetry directions.[29] However, that reasoning was based on the assumption that the Ti^{3+} ion was an isolated defect in the lattice. Our ENDOR results show that the Ti^{3+} ion in Chester's A center is not isolated.

Based on our direct ENDOR data, we assign the EPR signal in Fig. 1 (i.e., Chester's A center) to the neutral hydrogen donor. A model of this neutral hydrogen donor is constructed from the spin-Hamiltonian parameters in Table I. The 19.0° and 22.9° angles in Table I, associated with the *g* and hyperfine matrices, respectively, provide the critical information. Infrared absorption data from OH^- molecular ions in TiO_2 (rutile) show that the electric dipole lies in the basal plane of the crystal.[18,21] This is illustrated in Fig. 4 where the schematic representation of the donor has the unique axis of the OH^- molecular ion along the [$\bar{1}$10] direction in the basal plane. In the absence of lattice relaxation, the Ti^{3+} ion, the H^+ ion, and the O^{2-} ion in Fig. 4 are at the corners of a right triangle. Taking the OH^- bond length[30] to be 0.96 Å and the Ti-O separation distance to be 1.98 Å, the angle between the [110] direction and the line joining the Ti^{3+} and H^+ ions is 25.9°. This "predicted" angle is close to the 19.0° and 22.9° angles found in the experimental *g* and hyperfine matrices in Table I. These g_2 and A_2 principal-axis directions establish the model of the neutral hydrogen donor in TiO_2 (rutile) crystals.

The unpaired electron associated with the neutral charge state of the hydrogen donor is not centered on the hydrogen in an effective-mass-like wave function that spreads out over many shells of neighboring ions. Instead, the unpaired electron is localized, to a first approximation, on one titanium ion immediately adjacent to the OH^- ion. In other words, it is energetically more favorable to have the "extra" electron in a *d* orbital on the titanium ion than delocalized in a diffuse wave function centered on the hydrogen. In TiO_2 (rutile), there are three titanium ions that are nearest neighbors to a substitutional OH^- molecular ion. The two neighboring titanium ions along the [001] direction are equivalent, and they are slightly closer to the OH^- ion than the remaining titanium ion located along the [110] direction. In the unperturbed TiO_2 lattice at room temperature, these Ti-O distances are 1.9485 and 1.9800 Å, respectively. As we show in Fig. 4, the neutral hydrogen donor has the electron localized on the titanium ion along the [110] direction. In contrast, the neutral fluorine[13] donor in TiO_2 has the unpaired electron localized on one of the two equivalent titanium neighbors along the [001] direction. It is interesting that these two shallow donors have distinctly different minimum-energy ground state configurations in rutile TiO_2.

V. CONCLUSION

A detailed infrared absorption, EPR, and ENDOR study of hydrogen impurities in TiO_2 (rutile) bulk crystals is reported. As-grown crystals contain hydrogen donors in the form of isolated substitutional OH^- molecular ions. Changes in the charge state of these donors are easily achieved, and neutral hydrogen donors are observed after a slight reduction at high temperature in a nitrogen atmosphere or after photoexcitation with 442 nm light at low temperature. The angular dependence of the EPR and ENDOR spectra shows that the neutral hydrogen donor in this lattice consists of a substitutional Ti^{3+} ion adjacent to a substitutional OH^- ion. The hyperfine interaction with the participating hydrogen nucleus is unresolved in the EPR spectra but is clearly detected in ENDOR spectra. We suggest that the unpaired *d* electron on the Ti^{3+} ion occupies a $|x^2 - y^2\rangle$ orbital. The neutral hydrogen donor described in this paper corresponds to the often cited A center first reported by Chester.[6] Our results show that Chester's A center is not an interstitial Ti^{3+} ion.

ACKNOWLEDGMENTS

The authors wish to thank Greg W. Smith at the Air Force Institute of Technology for assistance in taking the infrared absorption data. This research was supported at West Virginia University by Grant No. DMR-0804352 from the National Science Foundation. The views expressed in this article are those of the authors and do not necessarily reflect the official policy or position of the Air Force, the Department of Defense, or the United States Government.

[1] C. Di Valentin, G. Pacchioni, and A. Selloni, J. Phys. Chem. C **113**, 20543 (2009).
[2] E. Finazzi, C. Di Valentin, and G. Pacchioni, J. Phys. Chem. C **113**, 3382 (2009).
[3] M. Bowker and R. A. Bennett, J. Phys.: Condens. Matter **21**, 474224 (2009).
[4] E. Finazzi, C. Di Valentin, G. Pacchioni, and A. Selloni, J. Chem. Phys. **129**, 154113 (2008).
[5] S. Wendt, P. T. Sprunger, E. Lira, G. K. H. Madsen, Z. Li, J. O. Hansen, J. Matthiesen, A. Blekinge-Rasmussen, E. Laegsgaard, B. Hammer, and F. Besenbacher, Science **320**, 1755 (2008).
[6] P. F. Chester, J. Appl. Phys. **32**, 2233 (1961).
[7] J. Kerssen and J. Volger, Physica (Amsterdam) **69**, 535 (1973).
[8] L. N. Shen, O. W. Johnson, W. D. Ohlsen, and J. W. DeFord, Phys. Rev. B **10**, 1823 (1974).
[9] M. Aono and R. R. Hasiguti, Phys. Rev. B **48**, 12406 (1993).
[10] S. Zhou, E. Cizmar, K. Potzger, M. Krause, G. Talut, M. Helm, J. Fassbender, S. A. Zvyagin, J. Wosnitza, and H. Schmidt, Phys. Rev. B **79**, 113201 (2009).
[11] Shan Yang, L. E. Halliburton, A. Manivannan, P. H. Bunton, D. B. Baker, M. Klemm, S. Horn, and A. Fujishima, Appl. Phys. Lett. **94**, 162114 (2009).
[12] F. D. Brandao, M. V. B. Pinheiro, G. M. Ribeiro, G. Medeiros-Rebeiro, and K. Krambrock, Phys. Rev. B **80**, 235204 (2009).
[13] S. Yang and L. E. Halliburton, Phys. Rev. B **81**, 035204 (2010).
[14] S. Yang, A. T. Brant, and L. E. Halliburton, Phys. Rev. B **82**, 035209 (2010).
[15] J.-M. Spaeth and H. Overhof, *Point Defects in Semiconductors and Insulators: Determination of Atomic and Electronic Structure from Paramagnetic Hyperfine Interactions*, Springer Series of Materials Science, Vol. 51 (Springer-Verlag, Berlin, 2003).
[16] F. Herklotz, E. V. Lavrov, and J. Weber, Phys. Rev. B **83**, 235202 (2011).
[17] B. H. Soffer, J. Chem. Phys. **35**, 940 (1961).
[18] O. W. Johnson, W. D. Ohlsen, and P. I. Kingsbury, Jr., Phys. Rev. **175**, 1102 (1968).
[19] J. R. Bates and R. A. Perkins, Phys. Rev. B **16**, 3713 (1977).
[20] Y. Chen, R. Gonzalez, and K. L. Tsang, Phys. Rev. Lett. **53**, 1077 (1984).
[21] S. Klauer and M. Wohlecke, EuroPhys. Lett. **20**, 439 (1992).
[22] M. Koudriachova, S. W. de Leeuw, and N. M. Harrison, Phys. Rev. B **70**, 165421 (2004).
[23] O. W. Johnson, J. DeFord, and J. W. Shaner, J. Appl. Phys. **44**, 3008 (1973).
[24] P. F. Chester, J. Appl. Phys. **32**, 866 (1961).
[25] P. H. Zimmermann, Phys. Rev. B **8**, 3917 (1973).
[26] Values of known Larmor frequencies at 350 mT are tabulated in Appendix A of J.-M. Spaeth, J. R. Niklas, and R. H. Bartram, *Structural Analysis of Point Defects in Solids: An Introduction to Multiple Magnetic Resonance Spectroscopy*, Springer Series in Solid-State Sciences, Vol. 43 Springer-Verlag, Berlin, 1992.
[27] H. J. Gerritsen, in *Paramagnetic Resonance*, edited by W. Low (Academic Press, New York, 1963) Vol. 1, p.3.
[28] W. Low and E. L. Offenbacher, in *Solid State Physics*, edited by F. Seitz and D. Turnbull (Academic Press, New York, 1965) Vol. **17**, p. 135.
[29] R. R. Hasiguti, Annu. Rev. Mater. Sci. **2**, 69 (1972).
[30] V. Szalay, L. Kovács, M. Wöhlecke, and E. Libowitzky, Chem. Phys. Lett. **354**, 56 (2002).